Light-induced excited spin-state trapping of Fe2+ observed by electron paramagnetic resonance of Mn2+

H. Daubric, R. Berger, Janis Kliava, Guillaume Chastanet, Olivier Nguyen, Jean-François Létard

Light-induced excited spin-state trapping of Fe^{2+} observed by electron paramagnetic resonance of Mn^{2+}

H. Daubric, R. Berger, and J. Kliava*
Centre de Physique Moléculaire Optique & Hertzienne, UMR Université Bordeaux I-CNRS 5798, 33405 Talence Cedex, France

G. Chastanet, O. Nguyen, and J.-F. Létard
Groupe des Sciences Moléculaires, Institut de Chimie de la Matière Condensée de Bordeaux, UPR CNRS 9048, 33608 Pessac Cedex, France

(Received 11 February 2002; published 19 August 2002)

We report an observation of the light-induced excited spin state trapping effect of Fe^{2+} ions using the electron paramagnetic resonance (EPR) technique. The experiment was carried out with a Mn^{2+}-containing molecular crystal of cis-bis(thiocyanato)-bis[(N-2′-pyridylmethylene)-4-(aminobiphenyl)]-iron(II) phase I. First, the photomagnetic properties of the compound were investigated in order to determine the experimental conditions for a complete low-to-high-spin photoconversion of the Fe^{2+} ions. The photoinduced high-spin fraction and the light-induced thermal Hysteresis studies under light irradiation at 830 nm show that a complete spin photoconversion occurs in the temperature range below 40 K. The Mn^{2+} EPR spectra recorded at these temperatures clearly show two different patterns corresponding to the low-spin state of Fe^{2+} (without light irradiation) and to the metastable high-spin state of this ion (under light irradiation), confirming the complete spin photoconversion. The values of the zero-field splitting parameter D for Mn^{2+} in the low-temperature light-induced high-spin structure are determined by computer simulations of the EPR spectra. These values corroborate the temperature dependence of D obtained using the superposition model for the high-spin state of the compound above the thermal hysteresis loop.

DOI: 10.1103/PhysRevB.66.054423 PACS number(s): 76.30.Fc, 78.20.Ls, 75.20.Ck

I. INTRODUCTION

The spin conversion phenomenon experienced by transition-metal ions with d^4-d^7 configurations in octahedral ligand fields was discovered by Cambi and Cagnasso[1] for an iron (III)-N,N-dialkyldithiocarbamate complex. Most of the spin conversion studies have been carried out on iron (II) molecular materials,[2,3] mainly because of their possible applications in molecular electronic devices. The spin conversion of the Fe^{2+} ion corresponds to a change of its electronic state from the ''normal'' paramagnetic high-spin state (HS, $S=2$) to the diamagnetic low-spin state (LS, $S=0$), and can be induced by an external perturbation such as temperature, pressure or light irradiation.[4] The later transformation, called light-induced excited spin state trapping (LIESST), first observed by Decurtins and co-workers,[5,6] is particularly promising for information storage. Indeed, as this phenomenon occurs on a molecular scale, one bit of information per molecule can be processed. Using two different light excitation wavelengths, data can be recorded by the LIESST effect and deleted by the reverse-LIESST effect.[7] Besides, in the absence of a crystallographic phase transition, the LS↔HS transformation occurs without fatigue. Actually, possible technical applications of the LIESST effect are limited, because the optical information can be stored with a sufficiently long lifetime only at low temperatures (typically, below *circa* 50 K). Various synthesis methods, technical characterizations and theoretical considerations are currently employed to identify the parameters which produce a shift of the limiting LIESST temperature towards the domain of potential applications.[8,9]

Among all experimental techniques (optical, magnetic, Mössbauer effect, etc.) used to study the spin transition and, in particular, the LIESST phenomenon, electron paramagnetic resonance (EPR) is of particular interest, owing to its sensitivity to both the magnetic state of the spin-changing ion and the crystalline structure of the compound. Meanwhile, the Fe^{2+} ion is ''EPR-silent'' not only in the diamagnetic LS state, but, in most cases of interest, also in the paramagnetic HS state, because of very short spin-lattice relaxation times and/or very large zero-field splitting. Fortunately, the thermal spin transition can be monitored by EPR in an *indirect* way by doping the compound with foreign paramagnetic ions—spin probes.[10–20] The advantage of the indirect EPR spectroscopy is to provide data not on (more or less trivial) *short-range* transformations in the close environment of the spin-changing ion but rather on concomitant *long-range* transformations involving the whole structure, and, consequently, on the cooperativity between structural units. Such data are particularly interesting, because the cooperativity is a *sine qua non* condition for the existence of a hysteresis loop, required for most technical applications. The Mn^{2+} ($3d^5$ configuration) ion is certainly the most appropriate paramagnetic probe for such studies, since its EPR spectra, exhibiting both zero-field splitting and hyperfine splitting, yield more data in comparison with other foreign paramagnetic ions. Besides, in the $^6S_{5/2}$ ground state of Mn^{2+}, no local structure distortion occurs, in contrast to the case, e.g., of the Jahn-Teller Cu^{2+} ion.[16]

To our knowledge, up to now only one (unsuccessful) attempt to observe the LIESST effect using the EPR has been

reported. That is, in Mn^{2+}-containing spin transition compounds $[Fe(bpp)_2][CF_3SO_3]_2 \cdot H_2O$ and $[Fe(bpp)_2][BF_4]_2$ [bpp= 2,6-bis(pyrazol-3-yl)pyridine] under a laser irradiation below the thermal spin transition region, Sung and McGarvey[17] observed a color change characteristic of the LS→HS conversion of Fe^{2+} ions but no change in the Mn^{2+} EPR spectrum. Consequently, these authors have inferred that, in contrast to the thermally induced spin transition, the low temperature light-induced LS→HS change produces no concomitant transformation in the crystal structure. It should be noted, however, that in this study the light irradiation was done outside the microwave cavity of EPR spectrometer, therefore, one cannot be sure that the HS→LS back conversion did not occur before recording the spectra. An EPR experiment with *in situ* light irradiation would certainly be more conclusive.

The present work deals with the cis-bis(thiocyanato)-bis[(N - 2′-pyridylmethylene) - 4 - (aminobiphenyl)]-iron(II), $[Fe(PM\text{-}BiA)_2(NCS)_2]$ molecular compound, a member of the $[Fe(PM\text{-}L)_2(NCS)_2]$ (L is a ligand) family.[21–24] This family is known for exhibiting very different types of magnetic behavior, from incomplete and gradual to complete and more or less abrupt spin transition with or without hysteresis. Among such compounds, the $[Fe(PM\text{-}BiA)_2(NCS)_2]$ phase I (Ref. 21) is particularly interesting, as far as it exhibits an extremely abrupt spin transition, occurring within 1–2 K, with a narrow hysteresis.

The crystal structure of $[Fe(PM\text{-}BiA)_2(NCS)_2]$ phase I has been determined by X-ray diffraction at 298 K (HS state) and 140 K (LS state).[21,24] In both spin states, this compound crystallizes in the *Pccn* space group and its molecular packing can be described as sheets of molecules parallel to the *ac* plane. The Fe^{2+} ions lay on a two-fold axis and are surrounded by three pairs of nitrogen atoms belonging, respectively, the first one to a NCS^- group in a *cis* position and the two remaining ones to the *PM-BiA* ligand. The HS→LS transition results in a shortening of the Fe-N bond lengths and a more regular FeN_6 core, all N-Fe-N angles converging to 90° in the LS state.

Preliminary EPR data on the temperature-induced spin transition have shown that in this compound (in the powder form) naturally doped with Mn^{2+} ions the apparent intensity of the *X*-band EPR spectra is much greater in the LS state than in the HS state of Fe^{2+} ions (due to a less important angular spread of resonance fields).[19,20] So it is clear that, in order to be observable by EPR, the light-induced LS→HS transition must be nearly complete. Meanwhile, the recently discovered light-induced thermal hysteresis (LITH) effect in cooperative spin-conversion compounds may limit the efficiency of the LS→HS photoconversion for a bulk sample.[21]

In this paper the photomagnetic properties of $[Fe(PM\text{-}BiA)_2(NCS)_2]$ phase I are first examined with the aim to determine the experimental conditions for a complete LS→HS photoconversion. Then, a LIESST experiment monitored by the Mn^{2+} EPR spectroscopy with an *in situ* light irradiation is described and discussed.

II. EXPERIMENT

Magnetic susceptibility measurements were carried with: (i) a Manics DSM-8 fully automatized Faraday-type magnetometer equipped with a DN-170 Oxford Instruments continuous-flow cryostat and a BE 15*f* Bruker electromagnet operating at *circa* 0.8 T and in the 80–300-K temperature range; and (ii) a MPMS-55 Quantum Design SQUID (superconducting quantum interferences device) magnetometer operating at *circa* 2 T in the 2–300-K temperature range. Data were corrected for the magnetization of the sample holder and for diamagnetic contributions. The LIESST experiments were carried out with the SQUID magnetometer coupled to an optical fiber diode laser (the excitation wavelength $\lambda_{exc} = 830 \pm 15$ nm) or a Kr^+ laser operating on single-line (532 nm) or multiline modes (647.7–676.4 nm). In order to obtain a complete spin conversion, a very thin layer of the compound was used in these experiments. Its weight was determined by comparing its thermal spin transition curve with that recorded with an accurately weighed bulk sample of the same compound. In order to prevent the sample heating, the laser power at the sample surface was limited to *circa* 5 mW/cm^2. Note that a local rise of the sample temperature would tend to decrease the magnetic response and, consequently, a jump of the signal would be detected when switching the light off, which has not been the case.

The *X*-band ($\nu \approx 9.3$ GHz) EPR spectra in the 10–177-K range were recorded with a Bruker EMX spectrometer provided with an ER4112HV variable temperature unit. The *Q*-band ($\nu \approx 34.8$ GHz) EPR spectra were recorded in the 114–293-K range with a Bruker ESP300 spectrometer supplied with an ER4121VT digital temperature control unit. The *X*-band EPR-monitored LIESST experiments were also carried out on a thin layer of the compound. The sample was deposited in a silica tube of a diameter of 4 mm connected to a T which allowed both a vacuum pumping and an *in situ* irradiation generated by an optical fiber coupled to a laser diode. The optical fiber was adjusted outside the EPR cavity in order to avoid producing a spurious resonance. The signal-to-noise ratio was improved by accumulating the EPR spectra of Mn^{2+} in the light-induced HS structure over 20 magnetic field sweeps.

III. PHOTOMAGNETIC PROPERTIES

Preliminary data on the photomagnetic properties of $[Fe(PM\text{-}BiA)_2(NCS)_2]$ phase I were obtained by irradiating the sample at 10 K with 532- or 647–676.4-nm wavelength light.[21] The limiting values of $\chi_M T$ (χ_M stands for the molar magnetic susceptibility and T for the temperature) reached under irradiation indicated an incomplete photoconversion of *circa* 20%. Recently it has been observed that light irradiation at 830 nm induces a complete LS→HS conversion. This has been attributed to the presence of a metal-to-ligand charge-transfer absorption band around 640 nm, hindering the light penetration in the bulk of the sample if the irradiation occurs in the visible spectral range.[25]

Figure 1 illustrates the magnetic and photomagnetic properties of the compound in a broad temperature range. The temperature-induced spin transition, shown in the high-temperature part, occurs with the characteristic temperatures (corresponding to equal amounts of HS and LS Fe^{2+} ions) $T_{1/2}\downarrow = 168$ K in the cooling mode and $T_{1/2}\uparrow = 173$ K in the

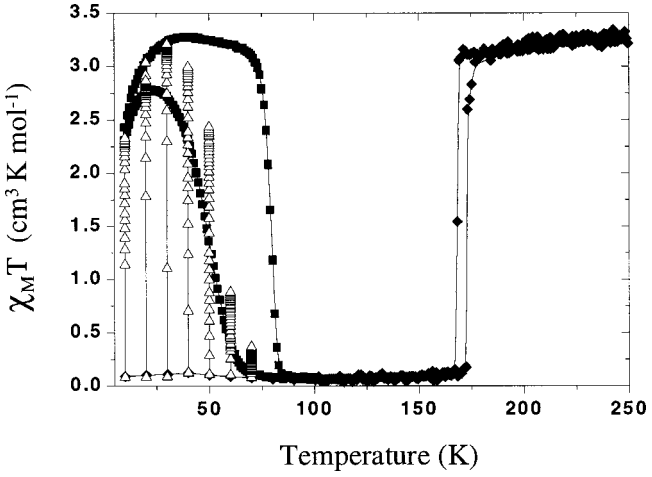

FIG. 1. Temperature dependence of the $\chi_M T$ product for powder sample of $[Fe(PM\text{-}BiA)_2(NCS)_2]$ phase I. The different symbols show data obtained: (◆) in the cooling and warming modes without irradiation (the thermally-induced spin transition with hysteresis), (△) with light irradiation at a fixed temperature, and (■) in the cooling and warming modes (0.3 K min^{-1}) after the light irradiation was applied for one hour, then turned off (the light-induced thermal hysteresis).

warming mode. The low-temperature part shows the photomagnetic response recorded at 830 nm in both the cooling and warming modes. The sample is first cooled down to 10 K without irradiation, so that a complete thermally induced HS→LS conversion of Fe^{2+} ions occurs. Next the sample is irradiated, and a rapid increase of the magnetic response is observed, confirming the LS→HS photoconversion. When the photostationary response is reached (usually after 1 h of irradiation), the sample is slowly (0.3 K/min) warmed up to 100 K and then cooled back to 10 K at the same rate. The LITH effect is clearly detected in this experience; the shape of the LITH curve in the cooling mode suggests that a complete photoinduced LS→HS conversion is reached only below 20 K. The LITH effect was also observed by Desaix *et al.*[26] in a $[Fe_xCo_{1-x}(btr)_2(NCS)_2]\cdot H_2O$ compound, and has been attributed to a competition between the constant photoexcitation and the self-accelerated thermal relaxation process. The shape of the LITH curve is strongly dependent on the irradiation procedure and particularly on the cooling rate. Figure 1 also shows irradiation experiments performed at 70, 60, 50, 40, 30, and 20 K. At a given temperature, the sample (initially in the LS state) is light irradiated until the saturation of the photomagnetic response. Between two consecutive measurement temperatures the sample is maintained for 5 min at 100 K in the dark in order to eliminate the photoinduced HS ion fraction. One can see that a complete photoinduced LS→HS conversion is reached for temperatures below *circa* 40 K.

IV. EPR DATA ON THE THERMALLY INDUCED TRANSITION

The previous EPR experiments have shown that the powder $[Fe(PM\text{-}BiA)_2(NCS)_2]$ phase I compound was naturally doped with 0.1% Mn/Fe.[19,20] Figure 2 illustrates EPR spectra series for the two microwave bands obtained in scanning the temperature range of the spin transition. The spectra only slightly change in cooling down from room temperature to the thermally induced spin transition temperature, then a striking change occurs in the range 174–171 K. At lower temperatures the spectra remain almost temperature-independent. In the warming mode the spectra gradually change from 20 to 174 K, then a marked transformation takes place between 174 and 177 K. Note the two quite different Mn^{2+} spectra patterns, corresponding to the HS and LS structures, observed at the same temperature in the warming and cooling modes. One can see that the thermal hysteresis is at least as clearly observed in the EPR spectra as in the magnetic susceptibility curve (cf. with the right part of Fig. 1).

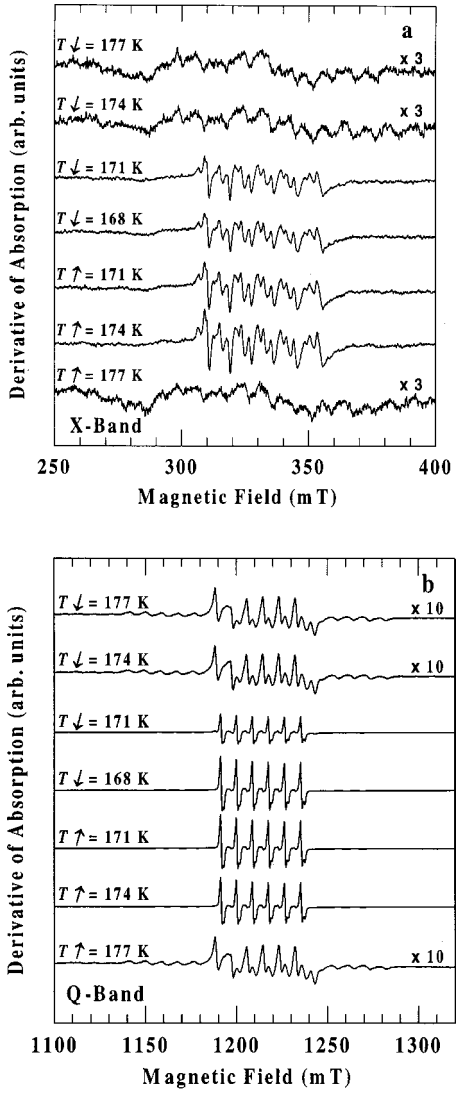

FIG. 2. Transformation of the *X*-band (a) and *Q*-band (b) EPR spectra of Mn^{2+}-containing spin transition compound $[Fe(PM\text{-}BiA)_2(NCS)_2]$ phase I in powder form. The temperature in the cooling ($T\downarrow$) and warming ($T\uparrow$) modes are shown alongside the curves.

The EPR spectra can be well described by the orthorhom-

bic spin Hamiltonian including only quadratic zero-field splitting (ZFS) terms, defined within the usual convention that $0 \leqslant \eta = 3E/D \leqslant 1$, and the hyperfine (HF) term

$$\mathcal{H} = g\beta \mathbf{B}\cdot\mathbf{S} + D\left[S_z^2 - \frac{1}{3}S(S+1)\right] + E(S_x^2 - S_y^2) + A\mathbf{S}\cdot\mathbf{I} \tag{1}$$

where $S = \frac{5}{2}$ and $I = \frac{5}{2}$, and all symbols have their usual meaning. In the *Q*-band spectra and in the *X*-band spectra corresponding to the LS state of Fe^{2+} the conditions $|D|, |E|, |A| \ll g\beta B$ hold with a good precision. A quantitative characterization of the EPR spectra transformations throughout the whole temperature range studied, including the spin transition region, has been obtained by numerical simulations using two different laboratory-developed computer simulation codes. The first one is based on Bir's version of the perturbation theory,[27,28] and allows taking into account all allowed ZFS components ($M \leftrightarrow M \pm 1$) and both allowed ($\Delta m = 0$) and forbidden ($\Delta m = \pm 1, \pm 2, \pm 3, \pm 4, \pm 5$) HF components with their corresponding intensities. (The latter components arise because, for comparable absolute values of ZFS and HF parameters, the selection rules governing the intensities of various HF transitions are broken down.[18,27,28]) However, the perturbation theory code could not be used to simulate *X*-band Mn^{2+} spectra in the HS compound, because of too high *D* parameter values in comparison with the *X*-band microwave quantum. So we have worked out a second simulation code, based on exact diagonalization of the spin Hamiltonian [Eq. (1)] matrix with no HF term; the latter one has been treated as a perturbation. This code is much more time consuming, so, for comparable computing times, it generates much more noisy spectra. Besides, the spectral features of the *X*-band HS-structure Mn^{2+} spectra, in contrast with the corresponding *Q*-band spectra, [cf. Figs. 2(a) and 2(b),] are rather poorly resolved because of a superposition of various ZFS components. On the other hand, owing to this superposition, the computer-generated spectra are particularly sensitive to the choice of the ZFS parameters. Indeed, in computer simulating the *X*-band HS-structure Mn^{2+} spectra with the exact diagonalization code, the best-fit parameters could be reliably deduced from the match of the main spectral feature positions.

The EPR spectra have been computer simulated according to the following expression:[28]

$$\mathcal{P}(B) = \sum_{M=-S+1}^{S} \sum_{m=-I}^{I} \sum_{\substack{\Delta m = 0 \\ |m+\Delta m| \leqslant I}}^{5} \times \int_0^{2\pi} \int_0^{\pi} W_{M,m,\Delta m} \left| \frac{dB_{M,m,\Delta m}}{d\nu} \right| \times F[B - B_{M,m,\Delta m}, \Delta B_{\mathrm{pp}}] \sin\vartheta \, d\vartheta \, d\varphi \tag{2}$$

where $W_{M,m,\Delta m}(D,E,\vartheta,\varphi)$ are the intensities of the corresponding transitions averaged over all directions of the microwave magnetic field and *F* is the line shape with a peak-to-peak linewidth ΔB_{pp} including broadening due to spin-lattice and spin-spin interactions as well as to static disorder,

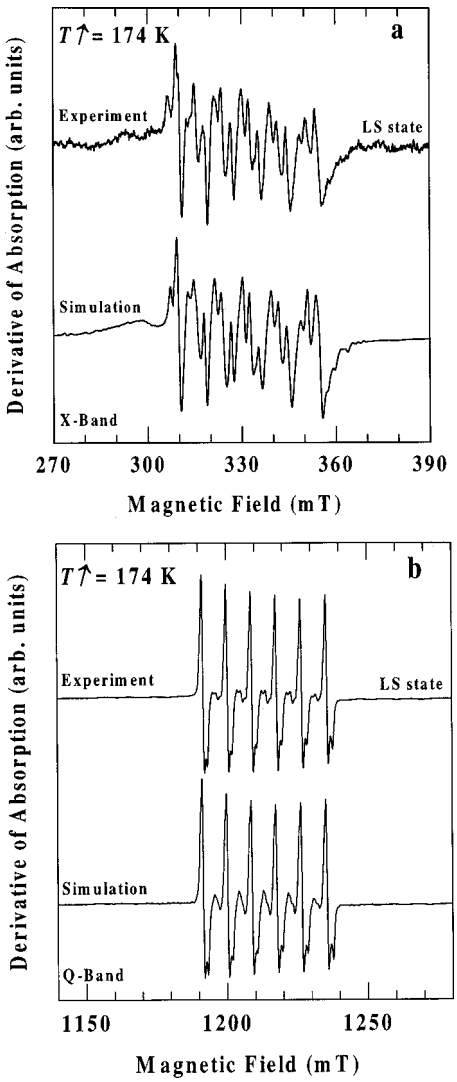

FIG. 3. Computer fits to the EPR spectra of Mn^{2+}-containing $[Fe(PM\text{-}BiA)_2(NCS)_2]$ phase I at 174 K in the warming mode (the LS state of Fe^{2+}) performed with the perturbation theory code in the *X* band (a) and the *Q* band (b). The simulation parameters are the same for the two bands, *viz.*, $g = 2.000$, $D = 162 \times 10^{-4}$ cm^{-1}, $E = 53 \times 10^{-4}$ cm^{-1}, $A = -82 \times 10^{-4}$ cm^{-1}, and $\Delta B_{\mathrm{pp}} = 0.25$ mT.

ϑ and φ are the polar and azimuthal angles of the static magnetic field **B** with respect to the axes of the spin Hamiltonian (1), $B_{M,m,\Delta m}(D,E,\vartheta,\varphi)$ are the resonance magnetic fields, and ν is the microwave frequency.

Figure 3 shows simulations of the Mn^{2+} EPR spectrum at 174 K in the warming mode (LS state of Fe^{2+}) using the perturbation theory code. Note that the same set of the simulation parameters has been used in both the *X* and *Q* bands. The close fits of the experimental EPR spectra obtained with spin Hamiltonian (1) justify the neglect of all other spin Hamiltonian terms, such as the quartic ZFS terms, as well as the nuclear Zeeman and nuclear quadrupole terms. Figure 4 shows the simulation results of the Mn^{2+} EPR spectrum in the HS state of Fe^{2+}: at 174 K in the cooling mode [(a) and (b)] and at room temperature (c). In the *Q*-band [(b) and (c)] very convincing fits are obtained. In the *X*-band spectrum (a), in spite of relatively high noise level in both the experimen-

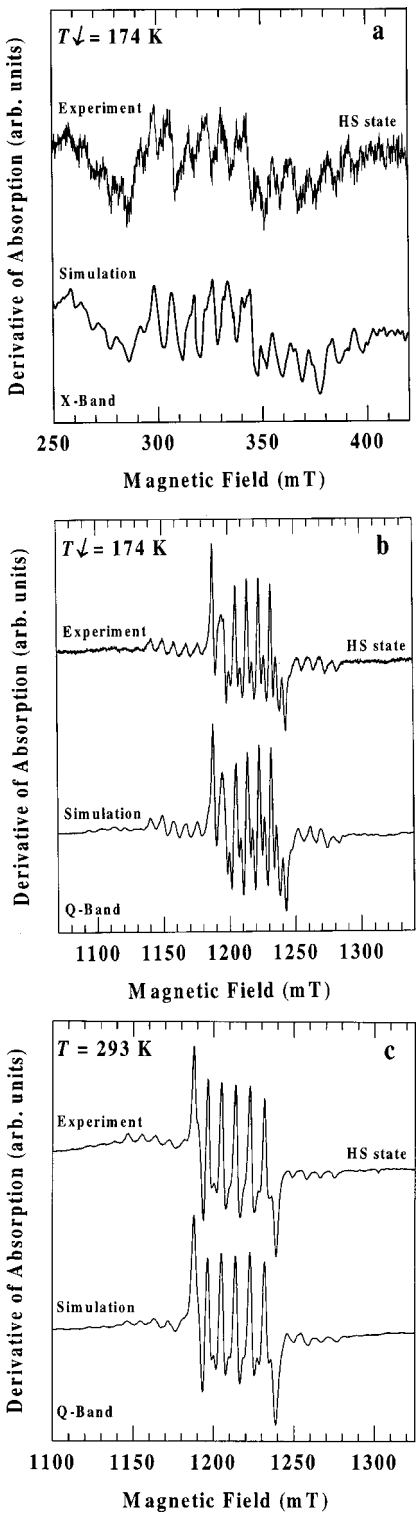

FIG. 4. Computer fits to the EPR spectrum of Mn^{2+}-containing $[Fe(PM\text{-}BiA)_2(NCS)_2]$ phase I in the HS state of Fe^{2+}: (a) At 174 K in the cooling mode in the *X* band (with the exact diagonalization code $D=420\times10^{-4}$ cm^{-1}, $E=17\times10^{-4}$ cm^{-1}, and $\Delta B_{pp}=1.0$ mT). (b) In the same conditions in the *Q* band (with the perturbation theory code and the same simulation parameters). (c) At room temperature in the *Q* band (with the perturbation theory code $D=310\times10^{-4}$ cm^{-1}, $E=31\times10^{-4}$ cm^{-1}, and $\Delta B_{pp}=1.1$ mT). In all cases, $g=2.000$ and $A=-82\times10^{-4}$ cm^{-1}.

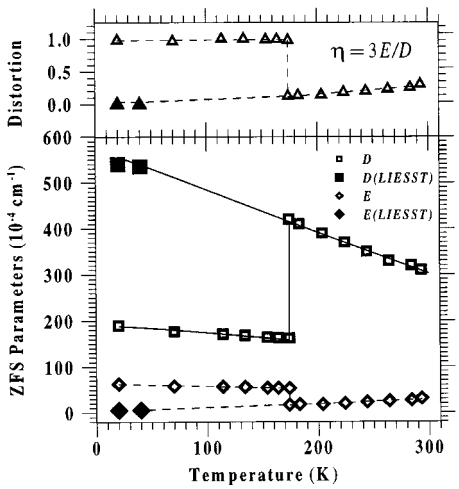

FIG. 5. Temperature dependence of the ZFS parameters for Mn^{2+} ions (symbols) in the two spin states of Fe^{2+} determined by computer simulations of the EPR spectra. The unfilled and filled symbols correspond, respectively, to the thermally induced spin transition and to the light-induced excited spin state of Fe^{2+}. The full lines are computer fits to the temperature dependence of the axial parameter *D* described by Eq. (3). The dashed lines are guides for the eyes.

tal and computer-generated spectra (the exact diagonalization code has been used here), the main features are satisfactorily reproduced with the same set of simulation parameters as in the *Q*-band spectrum at the same temperature (b).

The *g* factor and the HF constant *A* have been found isotropic with a good accuracy, $g=2.000\pm0.003$ and $A=(-82\pm1)\times10^{-4}$ cm^{-1}. These two values are not appreciably modified in the course of the spin transition; in contrast, quite significant changes occur in the ZFS parameters *D* and *E*. The temperature dependence of these parameters, as well as of the rhombic-to-axial parameter ratio $\eta=3E/D$, deduced from the computer simulations of the EPR spectra, are shown in Fig. 5. It follows that in the HS structure a quasiaxial symmetry is ''seen'' by the Mn^{2+} ion ($\eta\ll1$). On the other hand, in the LS structure the Mn^{2+} sites are subject to the maximal degree of rhombic distortion ($\eta\approx1$).

The intrinsic linewidth ΔB_{pp} is another essential EPR spectra characteristic significantly modified in the course of the LS→HS transition. Indeed, we have observed the increase of ΔB_{pp} from 0.2 mT in the LS state to 1 mT in the HS state due to the advent of magnetic interactions between Mn^{2+} and paramagnetic HS Fe^{2+} ions[20] [cf. the legends of Figs. 3 and 4 and of Figs. 7(a) and 7(b), *vide infra*].

Assuming that the Mn^{2+} paramagnetic probe substitutes for the Fe^{2+} ions, the temperature dependence of the axial ZFS parameter *D* can be obtained with the Newman superposition model[29] amended for contributions of thermal expansion of the crystal lattice and lattice vibrations.[30,31] We have fitted the $D(T)$ dependence, as obtained from the computer simulations, by the following expression:

$$D(T)=\frac{1}{2}\overline{b}_2(r_0)\sum_{i=1}^{6}\left[\frac{r_0}{r_i(T)}\right]^{t_2}(3\cos^2\vartheta_i-1)+D_{\nu0}\coth\frac{\Theta}{2T}. \tag{3}$$

The first term on the right-hand side of Eq. (3) is the standard superposition-model expression with $\overline{b_2}(r_0)$ an intrinsic parameter, $r_0 = 2.101$ Å a reference metal-ligand distance, $r_i(T)$ and ϑ_i the spherical coordinates of the ith ligand, and t_2 a power-law exponent. The second term accounts for the contribution of the lattice vibrations,[20,30,31] with $D_{\nu 0}$ proportional to the fundamental phonon frequency at $T = 0$ K, and Θ the Debye temperature. We assume that in a given spin state the local structure is temperature-independent with respect to the unit cell system, and we allow for a linear thermal expansion of the bond lengths between the metal ion and the jth ligand in proportion to the temperature expansion of the unit cell parameters.[20] The Debye temperature values in the LS and HS states are chosen as $\Theta_{LS} = 150$ K and $\Theta_{HS} = 130$ K, in accordance with those calculated by Boukheddaden and Varret for a similar compound $Fe(py)_2bipym(NCS)_2$.[32] With these assumptions, the best fit to the experimental $D(T)$ dependence is obtained for $D_{\nu 0} = -10 \times 10^{-4}$ cm^{-1}, $\overline{b_2}(r_0) = -120 \times 10^{-4}$ cm^{-1}, $t_2 = 4$, $D_{\nu 0} = -20 \times 10^{-4}$ cm^{-1}, $\overline{b_2}(r_0) = -220 \times 10^{-4}$ cm^{-1}, and $t_2 = 8$, respectively for the LS and HS states, as shown with full lines in Fig. 5. [These $D_{\nu 0}$ and $\overline{b_2}(r_0)$ values are somewhat different with respect to the previously quoted ones[20] because of the use of two distinct Debye temperatures for the two spin states.]

The reduction of the power law exponent t_2 in the LS state in comparison with the HS state is consistent with the decrease of the Fe-N bond lengths in the HS to LS transition. As far as the true metal-to-ligand distances are concerned, we note that in the sixfold coordination the ionic radius of the substituting spin probe Mn^{2+}, $R_{Mn^{2+}} = 0.97$ Å, is considerably different from those of the replaced Fe^{2+} ion in both the LS state, $R_{Fe^{2+}_{LS}} = 0.75$ Å and the HS state, $R_{Fe^{2+}_{HS}} = 0.92$ Å.[33] Therefore, the arrangement of the ligands of Mn^{2+} can be somewhat different from that of the Fe^{2+} ions. In particular, the change of the metal-to-ligand distances at the spin conversion temperature is certainly less pronounced for Mn^{2+}, since this ion does not undergo any transition at this temperature. Thus the Mn^{2+} ion is more tightly fitted to the less roomy LS Fe^{2+} sites than to the HS Fe^{2+} sites. One can conclude that the spin transition of Fe^{2+} induces considerable modifications not only in its own close environment but also in the whole crystal structure.

V. LIESST EFFECT OBSERVED BY EPR

The above findings show that the $[Fe(PM\text{-}BiA)_2(NCS)_2]$ phase I compound is a good candidate for a LIESST study using EPR spectroscopy. The experiment is carried out in the temperature range where the complete photoinduced LS→HS conversion has been reached, see Sec. III. The sample is first cooled down to a temperature well below the thermally induced spin transition region, *viz.*, 40, 30, 20, and 10 K. In the absence of light irradiation, the *X*-band EPR spectra recorded at these temperatures are characteristic of the LS compound structure [cf. Figs. 6(a) and 2(a)]. Next the sample is light irradiated at each above-mentioned temperature during *circa* 1 h. The EPR spectra

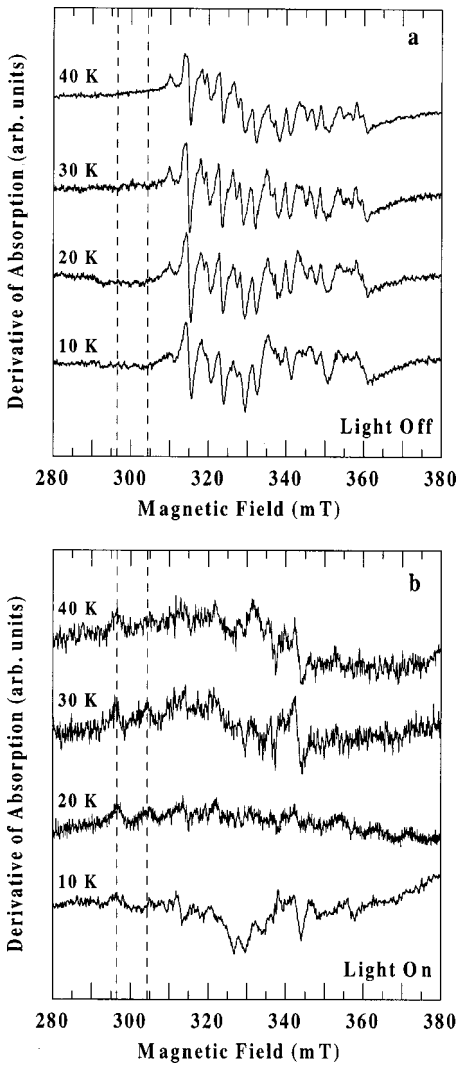

FIG. 6. Experimental *X*-band EPR spectra of Mn^{2+}-containing $[Fe(PM\text{-}BiA)_2(NCS)_2]$ phase I at the temperatures shown along side the curves: (a) after cooling down from room temperature without light irradiation; (b) after one hour of light irradiation.

measured just after the irradiation [Fig. 6(b)], show a dramatic change, their shape clearly corresponding to the HS structure. Between two successive low-temperature recordings the sample is warmed up to 100 K and the EPR spectra, recorded after cooling down again, recover the shape observed before the light irradiation. The reversibility of this spectra transformation provides one more proof of the fact that the EPR spectra recorded after light irradiation correspond to the HS structure.

In order to obtain a quantitative characterization of the light-induced *X*-band EPR spectra, they have been computer simulated. Figure 7 compares the simulation results of the experimental spectra recorded at 20 K without light irradiation [a LS state of Fe^{2+} (a)] and under light irradiation [a HS state of Fe^{2+} (b)]. Note a considerable (*circa* five times) increase of the intrinsic linewidth with respect to the spectrum corresponding to the LS state of Fe^{2+}. The relatively weak signal-to-noise ratio in the experimental Mn^{2+} EPR spectrum in the HS structure is due to the small amount of

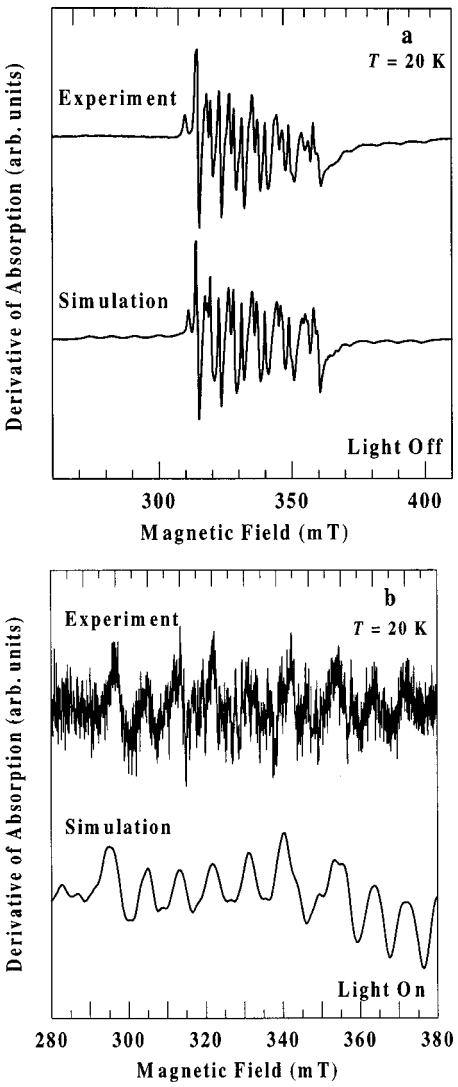

FIG. 7. Computer fits to the *X*-band EPR spectrum of Mn^{2+}-containing $[Fe(PM\text{-}BiA)_2(NCS)_2]$ phase I at 20 K: (a) Without light irradiation (the LS state of Fe^{2+}), the simulation parameters (obtained with the perturbation theory code) are $D=190\times10^{-4}$ cm^{-1}, $E=63\times10^{-4}$ cm^{-1}, and $\Delta B_{pp}=0.25$ mT. (b) Under light irradiation (the HS state of Fe^{2+}), the simulation parameters (obtained with the exact diagonalization code) are $D=540\times10^{-4}$ cm^{-1}, $E=5\times10^{-4}$ cm^{-1}, and $\Delta B_{pp}=1.25$ mT. In both cases, $g=2.000$ and $A=-82\times10^{-4}$ cm^{-1}.

the compound used in the experiment in order to obtain a complete light-induced spin conversion. Nevertheless, similarly to the case of high-temperature *X*-band Mn^{2+} spectrum in the HS structure [see Fig. 4(a)], all the main features in the experimental spectra are satisfactorily reproduced.

Finally, the ZFS parameters for Mn^{2+} ions in the HS structure, obtained in the EPR-monitored LIESST study under light irradiation, have been adjoined to Fig. 5 (filled symbols). Note that these data fit perfectly well the superposition-model predicted $D(T)$ dependence.

VI. CONCLUSION

This study reports the EPR observation of the LIESST effect. The photomagnetic properties of the $[Fe(PM\text{-}BiA)_2(NCS)_2]$ phase I (naturally doped with Mn^{2+}) were investigated in order to determine the experimental conditions for a complete LS→HS photoconversion of the Fe^{2+} ions. The LITH curve was recorded and the photoinduced HS fraction was followed in the 10–70 K temperature range. A complete photoconversion was obtained below 40 K with light irradiation at 830 nm. The EPR spectra recorded between 10 and 40 K without and with light irradiation unambiguously show a complete LS→HS photoconversion, in agreement with the photomagnetic study. The EPR spectra of the Mn^{2+} ions in the metastable low-temperature photoinduced HS structure were analyzed by computer simulations. The values of the ZFS parameter *D* in this structure match the $D(T)$ dependence predicted by the superposition model for the corresponding high-temperature HS structure.

The EPR study of the thermal spin transition shows the possibility of separately supervising the magnetic (spin-state) conversion and the related structural change by simultaneously monitoring the intrinsic linewidth and the spin Hamiltonian parameters. It would be interesting to carry out such a study on a spin-changing compound with a slow rate of the LS→HS structural transformation. In this case, a light irradiation at temperatures below the spin transition range would produce the HS state of a spin-changing ion in a LS crystalline structure. Thus, by recording time-resolved EPR spectra during light irradiation in the LIESST effect conditions, one could separately supervise the kinetics of the interrelated magnetic and structural transitions involved in this phenomenon.

ACKNOWLEDGMENTS

The authors are grateful to G. Villeneuve, Centre de Recherche Appliquée à l'Archéologie de Bordeaux, Université Bordeaux III, for assistance in carrying out the *Q*-band recordings, and to A. Bousseksou, Laboratoire de Chimie de Coordination, Toulouse, for helpful discussions.

*Corresponding author. Email address: jkliava@cribx1.u-bordeaux.fr

[1] L. Cambi and A. Cagnasso, Atti Accad. Naz. Lincei, Cl. Sci. Fis., Mat. Nat., Rend. **13**, 809 (1931).

[2] P. Gütlich, A. Hauser, and H. Spiering, Angew. Chem. Int. Ed. Engl. **33**, 2024 (1994).

[3] O. Kahn, *Molecular Magnetism* (VCH, New York, 1993).

[4] O. Kahn and C. J. Martinez, Science **279**, 44 (1988).

[5] S. Decurtins, P. Gütlich, C. P. Köhler, H. Spiering, and A. Hauser, Chem. Phys. Lett. **105**, 1 (1984).

[6] S. Decurtins, P. Gütlich, P. Hasselbach, A. Hauser, and H. Spiering, Inorg. Chem. **24**, 2174 (1985).

[7] A. Hauser, Chem. Phys. Lett. **124**, 543 (1986).

[8] J.-F. Létard, L. Capes, G. Chastenet, N. Moliner, S. Létard, J.-A. Real, and O. Kahn, Chem. Phys. Lett. **313**, 115 (1999).

[9] S. Marcén, L. Lecren, L. Capes, H. A. Goodwin, and J.-F. Létard,

Chem. Phys. Lett. **358**, 87 (2002).
[10] G. R. Hall and D. N. Hendrickson, Inorg. Chem. **15**, 607 (1976).
[11] P. S. Rao, A. Reuveni, B. R. McGarvey, P. Ganguli, and P. Gütlich, Inorg. Chem. **20**, 204 (1981).
[12] A. Ozarowski and B. R. McGarvey, Inorg. Chem. **28**, 2262 (1989).
[13] P. E. Daon and B. R. McGarvey, Inorg. Chem. **29**, 874 (1990).
[14] A. Ozarowski, Y. Shunzhong, B. R. McGarvey, A. Mislankar, and J. E. Drake, Inorg. Chem. **30**, 3167 (1991).
[15] Y. Servant, C. Cantin, O. Kahn, and J. Kliava, in *Modern Applications of EPR/ESR* (Springer, Singapore, 1997), p. 346.
[16] C. Cantin, H. Daubric, J. Kliava, and O. Kahn, Solid State Commun. **108**, 17 (1998).
[17] R. C. W. Sung and B. R. McGarvey, Inorg. Chem. **38**, 3644 (1999).
[18] H. Daubric, C. Cantin, C. Thomas, J. Kliava, J.-F. Létard, and O. Kahn, Chem. Phys. Lett. **244**, 75 (1999).
[19] J.-F. Létard, H. Daubric, C. Cantin, Y. A. Bouhedja, J. Kliava, O. Nguyen, and O. Kahn, Mol. Cryst. Liq. Cryst. **335**, 1207 (1999).
[20] H. Daubric, J. Kliava, P. Guionneau, D. Chasseau, J.-F. Létard, and O. Kahn, J. Phys.: Condens. Matter **12**, 5481 (2000).
[21] J.-F. Létard, P. Guionneau, L. Rabardel, J. A. K. Howard, A. E. Goeta, D. Chasseau, and O. Kahn, Inorg. Chem. **37**, 4432 (1998).
[22] J.-F. Létard, P. Guionneau, E. Codjovi, O. Lavastre, G. Bravic, D. Chasseau, and O. Kahn, J. Am. Chem. Soc. **119**, 10 861 (1997).
[23] P. Guionneau, J.-F. Létard, D. S. Yufit, D. Chasseau, G. Bravic, A. E. Goeta, J. A. K. Howard, and O. Kahn, J. Mater. Chem. **9**, 985 (1999).
[24] V. Ksenofontov, G. Levchenko, H. Spiering, P. Gütlich, J.-F. Létard, Y. A. Bouhedja, and O. Kahn, Chem. Phys. Lett. **294**, 545 (1998).
[25] S. Montant, G. Chastanet, E. Freysz, and J.-F. Létard (unpublished).
[26] A. Desaix, O. Roubeau, J. Jeftic, J. G. Haasnaoot, K. Boukheddaden, E. Codjovi, J. Linares, M. Nogues, and F. Varret, Eur. Phys. J. B **6**, 183 (1998).
[27] G. L. Bir, Fiz. Tverd. Tela (Leningrad) **5**, 2236 (1963) [Sov. Phys. Solid State **5**, 1628 (1964)].
[28] J. Kliava, Phys. Status Solidi B **134**, 411 (1986).
[29] D. J. Newman, Adv. Phys. **21**, 197 (1971).
[30] A. Leclerc and A. Manoogian, J. Chem. Phys. **63**, 4456 (1975).
[31] R. J. Gleason, J. L. Boldú, E. Cabrera, C. Quintanar, and P. E. Muñoz, J. Phys. Chem. Solids **58**, 1507 (1997).
[32] K. Boukheddaden and F. Varret, Hyperfine Interact. **72**, 349 (1992).
[33] R. D. Shannon, Acta Crystallogr., Sect. A: Cryst. Phys., Diffr., Theor. Gen. Crystallogr. **32**, 751 (1976).